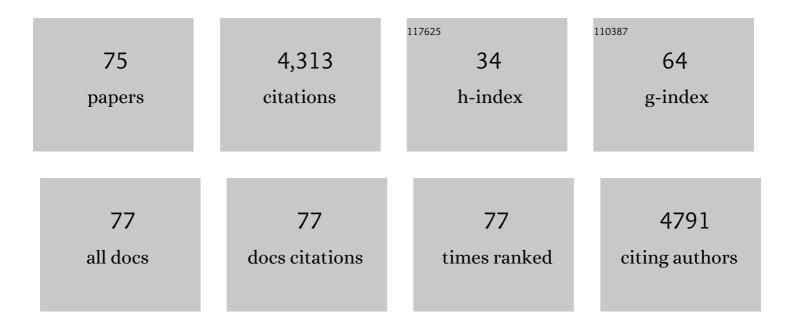
List of Publications by Year in descending order

Source: https://exaly.com/author-pdf/4876342/publications.pdf Version: 2024-02-01



#	Article	IF	CITATIONS
1	Hyperpolarized Micro-NMR Platform for Sensitive Analysis of In Vitro Metabolic Flux in Living Cells. Methods in Molecular Biology, 2022, 2393, 561-569.	0.9	0
2	Ketohexokinase-mediated fructose metabolism is lost in hepatocellular carcinoma and can be leveraged for metabolic imaging. Science Advances, 2022, 8, eabm7985.	10.3	9
3	Hyperpolarized [5- ¹³ C,4,4- ² H ₂ ,5- ¹⁵ N]-L-glutamine provides a means of annotating inÂvivo metabolic utilization of glutamine. Proceedings of the National Academy of Sciences of the United States of America, 2022, 119, e2120595119.	7.1	8
4	Metabolic analysis as a driver for discovery, diagnosis, and therapy. Cell, 2022, 185, 2678-2689.	28.9	51
5	Multiâ€sample measurement of hyperpolarized pyruvateâ€ŧoâ€ŀactate flux in melanoma cells. NMR in Biomedicine, 2021, 34, e4447.	2.8	6
6	High Fructose Drives the Serine Synthesis Pathway in Acute Myeloid Leukemic Cells. Cell Metabolism, 2021, 33, 145-159.e6.	16.2	34
7	Dynamic volumetric hyperpolarized ¹³ C imaging with multiâ€echo EPI. Magnetic Resonance in Medicine, 2021, 85, 978-986.	3.0	3
8	Editorial commentary for the special issue: technological developments in hyperpolarized 13C imaging—toward a deeper understanding of tumor metabolism in vivo. Magnetic Resonance Materials in Physics, Biology, and Medicine, 2021, 34, 1-3.	2.0	3
9	Immunometabolism of Tissue-Resident Macrophages – An Appraisal of the Current Knowledge and Cutting-Edge Methods and Technologies. Frontiers in Immunology, 2021, 12, 665782.	4.8	15
10	Imaging Early Response to Checkpoint Inhibition. Cancer Research, 2021, 81, 3444-3445.	0.9	0
11	Deuterium Metabolic Imaging of Pancreatic Cancer. NMR in Biomedicine, 2021, 34, e4603.	2.8	4
12	The metabolic adaptation evoked by arginine enhances the effect of radiation in brain metastases. Science Advances, 2021, 7, eabg1964.	10.3	18
13	Hyaluronic acid fuels pancreatic cancer cell growth. ELife, 2021, 10, .	6.0	45
14	Hyperpolarized MRI of Human Prostate Cancer Reveals Increased Lactate with Tumor Grade Driven by Monocarboxylate Transporter 1. Cell Metabolism, 2020, 31, 105-114.e3.	16.2	100
15	Limited Environmental Serine and Glycine Confer Brain Metastasis Sensitivity to PHGDH Inhibition. Cancer Discovery, 2020, 10, 1352-1373.	9.4	145
16	Elevated Tumor Lactate and Efflux in High-grade Prostate Cancer demonstrated by Hyperpolarized 13C Magnetic Resonance Spectroscopy of Prostate Tissue Slice Cultures. Cancers, 2020, 12, 537.	3.7	14
17	Hyperpolarized [6- ¹³ C, ¹⁵ N ₃]-Arginine as a Probe for <i>in Vivo</i> Arginase Activity. ACS Chemical Biology, 2019, 14, 665-673.	3.4	15
18	The Role of Lactate Metabolism in Prostate Cancer Progression and Metastases Revealed by Dual-Agent Hyperpolarized 13C MRSI. Cancers, 2019, 11, 257.	3.7	41

#	Article	IF	CITATIONS
19	Hyperpolarized 13C MRI: Path to Clinical Translation in Oncology. Neoplasia, 2019, 21, 1-16.	5.3	316
20	Hyperpolarized MRI Visualizes Warburg Effects and Predicts Treatment Response to mTOR Inhibitors in Patient-Derived ccRCC Xenograft Models. Cancer Research, 2019, 79, 242-250.	0.9	27
21	Targeted AKT Inhibition in Prostate Cancer Cells and Spheroids Reduces Aerobic Glycolysis and Generation of Hyperpolarized [1-13C] Lactate. Molecular Cancer Research, 2018, 16, 453-460.	3.4	16
22	Metabolic Imaging of the Human Brain with Hyperpolarized 13C Pyruvate Demonstrates 13C Lactate Production in Brain Tumor Patients. Cancer Research, 2018, 78, 3755-3760.	0.9	179
23	Imaging glutathione depletion in the rat brain using ascorbate-derived hyperpolarized MR and PET probes. Scientific Reports, 2018, 8, 7928.	3.3	20
24	A non-synthetic approach to extending the lifetime of hyperpolarized molecules using D2O solvation. Journal of Magnetic Resonance, 2018, 295, 57-62.	2.1	13
25	Biomarker-Based PET Imaging of Diffuse Intrinsic Pontine Glioma in Mouse Models. Cancer Research, 2017, 77, 2112-2123.	0.9	27
26	Hyperpolarized 13C Spectroscopic Evaluation of Oxidative Stress in a Rodent Model of Steatohepatitis. Scientific Reports, 2017, 7, 46014.	3.3	15
27	Real-time quantitative analysis of metabolic flux in live cells using a hyperpolarized micromagnetic resonance spectrometer. Science Advances, 2017, 3, e1700341.	10.3	47
28	Multinuclear NMR and MRI Reveal an Early Metabolic Response to mTOR Inhibition in Sarcoma. Cancer Research, 2017, 77, 3113-3120.	0.9	18
29	Hyperpolarized 13 C pyruvate mouse brain metabolism with absorptive-mode EPSI at 1 T. Journal of Magnetic Resonance, 2017, 275, 120-126.	2.1	12
30	InÂVivo Imaging of Glutamine Metabolism to the Oncometabolite 2-Hydroxyglutarate in IDH1/2 Mutant Tumors. Cell Metabolism, 2017, 26, 830-841.e3.	16.2	82
31	Noninvasive Interrogation of Cancer Metabolism with Hyperpolarized ¹³ C MRI. Journal of Nuclear Medicine, 2017, 58, 1201-1206.	5.0	20
32	Cancer Metabolism and Tumor Heterogeneity: Imaging Perspectives Using MR Imaging and Spectroscopy. Contrast Media and Molecular Imaging, 2017, 2017, 1-18.	0.8	39
33	Hyperpolarization MRI. Topics in Magnetic Resonance Imaging, 2016, 25, 31-37.	1.2	19
34	Separation of extra- and intracellular metabolites using hyperpolarized 13C diffusion weighted MR. Journal of Magnetic Resonance, 2016, 270, 115-123.	2.1	19
35	Sampling Hyperpolarized Molecules Utilizing a 1 Tesla Permanent Magnetic Field. Scientific Reports, 2016, 6, 32846.	3.3	14
36	High-Throughput Indirect Quantitation of ¹³ C Enriched Metabolites Using ¹ H NMR. Analytical Chemistry, 2016, 88, 11147-11153.	6.5	13

#	Article	IF	CITATIONS
37	Non-invasive PET Imaging of PARP1 Expression in Glioblastoma Models. Molecular Imaging and Biology, 2016, 18, 386-392.	2.6	70
38	Remodeling the Vascular Microenvironment of Glioblastoma with α-Particles. Journal of Nuclear Medicine, 2016, 57, 1771-1777.	5.0	25
39	Caged [¹⁸ F]FDG Glycosylamines for Imaging Acidic Tumor Microenvironments Using Positron Emission Tomography. Bioconjugate Chemistry, 2016, 27, 170-178.	3.6	38
40	The Potential of Metabolic Imaging. Seminars in Nuclear Medicine, 2016, 46, 28-39.	4.6	31
41	Non-Invasive Differentiation of Benign Renal Tumors from Clear Cell Renal Cell Carcinomas Using Clinically Translatable Hyperpolarized 13C Pyruvate Magnetic Resonance. Tomography, 2016, 2, 35-42.	1.8	26
42	Metabolic response of prostate cancer to nicotinamide phophoribosyltransferase inhibition in a hyperpolarized MR/PET compatible bioreactor. Prostate, 2015, 75, 1601-1609.	2.3	30
43	13C-labeled biochemical probes for the study of cancer metabolism with dynamic nuclear polarization-enhanced magnetic resonance imaging. Cancer & Metabolism, 2015, 3, 9.	5.0	36
44	Novel Approaches to Imaging Tumor Metabolism. Cancer Journal (Sudbury, Mass), 2015, 21, 165-173.	2.0	27
45	Realâ€ŧime measurement of hyperpolarized lactate production and efflux as a biomarker of tumor aggressiveness in an MR compatible 3D cell culture bioreactor. NMR in Biomedicine, 2015, 28, 1141-1149.	2.8	43
46	Rapid in vivo apparent diffusion coefficient mapping of hyperpolarized ¹³ C metabolites. Magnetic Resonance in Medicine, 2015, 74, 622-633.	3.0	27
47	Noninvasive In Vivo Imaging of Diabetes-Induced Renal Oxidative Stress and Response to Therapy Using Hyperpolarized 13C Dehydroascorbate Magnetic Resonance. Diabetes, 2015, 64, 344-352.	0.6	59
48	Chemistry and biochemistry of ¹³ C hyperpolarized magnetic resonance using dynamic nuclear polarization. Chemical Society Reviews, 2014, 43, 1627-1659.	38.1	308
49	OCT1 is a high-capacity thiamine transporter that regulates hepatic steatosis and is a target of metformin. Proceedings of the National Academy of Sciences of the United States of America, 2014, 111, 9983-9988.	7.1	203
50	A Boronate-Caged [¹⁸ F]FLT Probe for Hydrogen Peroxide Detection Using Positron Emission Tomography. Journal of the American Chemical Society, 2014, 136, 14742-14745.	13.7	113
51	Diffusion MR of hyperpolarized 13C molecules in solution. Analyst, The, 2013, 138, 1011.	3.5	31
52	Hyperpolarized 13C-Pyruvate Magnetic Resonance Reveals Rapid Lactate Export in Metastatic Renal Cell Carcinomas. Cancer Research, 2013, 73, 529-538.	0.9	95
53	Solid phase synthesis of hydroxamate peptides for histone deacetylase inhibition. Tetrahedron Letters, 2013, 54, 151-153.	1.4	6
54	Effect of Oxygen Concentration on Viability and Metabolism in a Fluidized-Bed Bioartificial Liver Using ³¹ P and ¹³ C NMR Spectroscopy. Tissue Engineering - Part C: Methods, 2013, 19, 93-100.	2.1	13

#	Article	IF	CITATIONS
55	Hyperpolarized [1- ¹³ C]Dehydroascorbate MR Spectroscopy in a Murine Model of Prostate Cancer: Comparison with ¹⁸ F-FDG PET. Journal of Nuclear Medicine, 2013, 54, 922-928.	5.0	50
56	Metabolic Reprogramming and Validation of Hyperpolarized ¹³ C Lactate as a Prostate Cancer Biomarker Using a Human Prostate Tissue Slice Culture Bioreactor. Prostate, 2013, 73, 1171-1181.	2.3	93
57	Generating contrast in hyperpolarized 13C MRI using ligand–receptor interactions. Analyst, The, 2012, 137, 3427.	3.5	20
58	A Hydrogen Peroxide-Responsive Hyperpolarized ¹³ C MRI Contrast Agent. Journal of the American Chemical Society, 2011, 133, 3776-3779.	13.7	97
59	In vivo measurement of normal rat intracellular pyruvate and lactate levels after injection of hyperpolarized [1-13C]alanine. Magnetic Resonance Imaging, 2011, 29, 1035-1040.	1.8	34
60	Imaging of blood flow using hyperpolarized [¹³ C]Urea in preclinical cancer models. Journal of Magnetic Resonance Imaging, 2011, 33, 692-697.	3.4	105
61	Hyperpolarized ¹³ C dehydroascorbate as an endogenous redox sensor for in vivo metabolic imaging. Proceedings of the National Academy of Sciences of the United States of America, 2011, 108, 18606-18611.	7.1	143
62	Metabolic assessment of a novel chronic myelogenous leukemic cell line and an imatinib resistant subline by 1H NMR spectroscopy. Metabolomics, 2010, 6, 439-450.	3.0	20
63	Metabolic, pathologic, and genetic analysis of prostate tissues: quantitative evaluation of histopathologic and mRNA integrity after HR-MAS spectroscopy. NMR in Biomedicine, 2010, 23, 391-398.	2.8	32
64	Hyperpolarized ¹³ C spectroscopy and an NMRâ€compatible bioreactor system for the investigation of realâ€time cellular metabolism. Magnetic Resonance in Medicine, 2010, 63, 322-329.	3.0	67
65	Multi-compound polarization by DNP allows simultaneous assessment of multiple enzymatic activities in vivo. Journal of Magnetic Resonance, 2010, 205, 141-147.	2.1	154
66	Generation of hyperpolarized substrates by secondary labeling with [1,1-13C] acetic anhydride. Proceedings of the National Academy of Sciences of the United States of America, 2009, 106, 5503-5507.	7.1	46
67	Evaluation of the ERETIC method as an improved quantitative reference for ¹ H HRâ€MAS spectroscopy of prostate tissue. Magnetic Resonance in Medicine, 2009, 61, 525-532.	3.0	62
68	Hyperpolarized [2- ¹³ C]-Fructose: A Hemiketal DNP Substrate for In Vivo Metabolic Imaging. Journal of the American Chemical Society, 2009, 131, 17591-17596.	13.7	106
69	¹ H HRâ€MAS spectroscopy for quantitative measurement of choline concentration in amniotic fluid as a marker of fetal lung maturity: Inter―and intraobserver reproducibility study. Journal of Magnetic Resonance Imaging, 2008, 28, 1540-1545.	3.4	18
70	Quantification of choline―and ethanolamine ontaining metabolites in human prostate tissues using ¹ H HRâ€MAS total correlation spectroscopy. Magnetic Resonance in Medicine, 2008, 60, 33-40.	3.0	110
71	Evaluation of lactate and alanine as metabolic biomarkers of prostate cancer using ¹ H HRâ€MAS spectroscopy of biopsy tissues. Magnetic Resonance in Medicine, 2008, 60, 510-516.	3.0	189
72	Lactic Acid and Proteoglycans as Metabolic Markers for Discogenic Back Pain. Spine, 2008, 33, 312-317.	2.0	60

#	Article	IF	CITATIONS
73	Quantitative analysis of prostate metabolites using1H HR-MAS spectroscopy. Magnetic Resonance in Medicine, 2006, 55, 1257-1264.	3.0	242
74	Correlation of HR-MAS Spectroscopy Derived Metabolite Concentrations With Collagen and Proteoglycan Levels and Thompson Grade in the Degenerative Disc. Spine, 2005, 30, 2683-2688.	2.0	31
75	Characterization of intervertebral disc degeneration by high-resolution magic angle spinning (HR-MAS) spectroscopy. Magnetic Resonance in Medicine, 2005, 53, 519-527.	3.0	44